

Cite this: *RSC Sustainability*, 2026, 4, 1943

# Boosting the reactivity of crystalline cellulose by a cold base treatment for catalytic hydrolysis with a carbon-based catalyst

Naomi Nishimura,<sup>a</sup> Yoichi Masui,<sup>a</sup> Ryo Shimane,<sup>b</sup> Shunsaku Yasumura,<sup>c</sup> Tomohiro Iwai,<sup>a</sup> Masaru Ogura,<sup>c</sup> and Hirokazu Kobayashi<sup>\*ad</sup>

Hydrolysis of cellulose to glucose is an essential step in the second-generation biorefinery. However, the robust structure of cellulose I, the predominant crystalline allomorph in nature, has hampered this reaction. Increasing the reactivity of cellulose in an efficient manner alleviates this issue. This work demonstrates that treating cellulose I with an 18 wt% NaOH aqueous solution at low temperatures improves its reactivity. The treatment below  $-28\text{ }^{\circ}\text{C}$ , liquidus temperature of the solution, elevated the yield of glucose 2.2 times in its hydrolysis reaction with a carbon-based catalyst developed for crystalline cellulose hydrolysis. Characterization of the cellulose samples has indicated that the NaOH treatment not only transforms the crystalline form into cellulose II but also, particularly at low temperatures, disrupts the hydrogen-bonding network of cellulose without affecting the macro-scale order of cellulose molecules in the cellulose II structure. This is a facile method to increase the reactivity of cellulose.

Received 24th December 2025

Accepted 3rd March 2026

DOI: 10.1039/d5su00951k

rsc.li/rscsus

## Sustainability spotlight

Current chemical production mostly relies on fossil resources, which should be altered to renewable resources towards Sustainable Development Goals, especially for Goal 12 “Responsible Consumption and Production”. Cellulose is the most abundant organic renewable resource, but its efficient conversion is a formidable challenge. This is due to the recalcitrance of the natural cellulose, which has a densely-packed crystalline form. Our work shows that just decreasing the temperature of a commercially established process (mercerization) improves the reactivity of cellulose, giving a 2.2-fold higher yield of glucose in its hydrolysis. We have also clarified why low-temperature treatment enhances the reactivity. This finding helps the development of sustainable chemistry.

## Introduction

Cellulose is a main component of woody biomass and the most abundant carbohydrate. The use of cellulose is a promising strategy for replacing fossil resources in the production of chemicals.<sup>1</sup> A common process for utilizing cellulose is hydrolysis to glucose. The hydrolysis reaction requires a catalyst, but the catalyst barely accesses to the surface or inside of cellulose due to the rigid structure of cellulose,<sup>2</sup> resulting in slow or non-selective reactions.

A potential methodology to address this issue is improving the reactivity of cellulose. Cellulose shows crystal polymorphism, with natural cellulose existing in the cellulose I

structure. Cellulose molecules are aligned in the same direction and densely packed with rigid hydrogen bonds such as O3...HO6 (Fig. 1a) and dispersion forces,<sup>3</sup> resulting in high resistance to hydrolysis reactions.<sup>2</sup> Therefore, the transformation of cellulose I to other crystalline structures is an option for this purpose.<sup>4-6</sup> A cost-efficient method is mercerization, in which cellulose I transforms into the cellulose II allomorph just by dipping in a NaOH aqueous solution.<sup>6</sup> This method is widely used in the textile industry for better luster and dyeability. Cellulose II shows a higher reactivity than cellulose I in both enzymatic and acid hydrolysis reactions.<sup>4-6</sup> Adjacent cellulose molecules in the cellulose II crystal are arranged antiparallel, and O2 and O6 play major roles in forming intermolecular hydrogen bonds (Fig. 1b).<sup>5</sup> While cellulose I has two hydrogen bonds surrounding each glycosidic bond, cellulose II forms only one bond, leaving one side open. This is a possible cause of the higher reactivity.

The treating temperature is a considerable factor in mercerization. Low-temperature mercerization (4 to  $-40\text{ }^{\circ}\text{C}$ ) provides better transformation of cellulose I to cellulose II.<sup>5,7-9</sup> Therefore, low-temperature mercerization is a potential methodology for improving cellulose reactivity.

<sup>a</sup>Department of Basic Science, Graduate School of Arts and Sciences, The University of Tokyo, 3-8-1 Komaba, Meguro-Ku, Tokyo 153-8902, Japan. E-mail: kobayashi-hi@g.ecc.u-tokyo.ac.jp

<sup>b</sup>Department of Chemistry and Biotechnology, School of Engineering, The University of Tokyo, 7-3-1 Hongo, Bunkyo-Ku, Tokyo 113-8656, Japan

<sup>c</sup>Institute of Industrial Science, The University of Tokyo, 4-6-1 Komaba, Meguro-Ku, Tokyo 153-8505, Japan

<sup>d</sup>Komaba Institute for Science, Graduate School of Arts and Sciences, The University of Tokyo, 3-8-1 Komaba, Meguro-Ku, Tokyo 153-8902, Japan



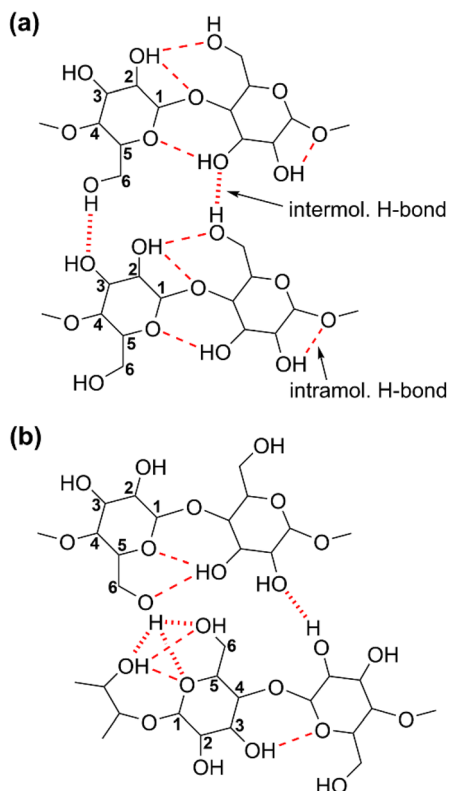


Fig. 1 Hydrogen-bonding structures of crystalline cellulose allomorphs. (a) Cellulose I. (b) Cellulose II.

In this work, we found that mercerization pretreatment at a low temperature below  $-28\text{ }^{\circ}\text{C}$  enhances the reactivity of cellulose, achieving nearly twice the reactivity compared with treatment at room temperature. The improved reactivity was not due to a better transformation to cellulose II but due to the disruption of hydrogen bonds. Characterization of mercerized cellulose prepared at different temperatures showed that the samples were in the cellulose II form with similar crystallinity, as revealed by X-ray diffraction (XRD) analysis, regardless of the treatment temperature. However, nuclear magnetic resonance (NMR) spectroscopy indicated disordered hydrogen bonding structures in the low-temperature treatment samples. Accordingly, the low-temperature treatment preserves the molecular arrangement of cellulose II roughly, but disrupts hydrogen bonds, which accounts for the improved reactivity. Just decreasing the temperature in the common pretreatment brings out its potential to improve cellulose reactivity.

## Experimental

### Reagents

Microcrystalline cellulose (Avicel PH-101, Merck),  $\text{HNO}_3$  (60 wt%, guaranteed reagent, Nacalai Tesque),  $\text{H}_2\text{SO}_4$  (95 wt%, guaranteed reagent, Nacalai Tesque) and  $\text{NaOH}$  (97 wt%, guaranteed reagent, Nacalai Tesque) were used without further purification. Water was purified using a WEX3NUV system (Yamato Scientific) equipped with a reverse osmosis membrane, an electrodeionization cell and a UV lamp (254 nm).

### Preparation of the catalyst named Cel-cat

We followed the procedure reported in the literature.<sup>10</sup> 10 g of Avicel in a Pyrex dish (90 mm diameter) was placed in an oven (FP100, Yamato Scientific), heated at a ramp rate of  $5\text{ }^{\circ}\text{C min}^{-1}$  to  $300\text{ }^{\circ}\text{C}$  and then kept at that temperature for 4 h. A black powder of 1.7 g (17 wt% yield) was obtained. That sample (2.0 g) was put into a 200 mL Pyrex beaker together with 40 mL of  $\text{HNO}_3$ . The beaker was immersed in an oil bath at  $180\text{ }^{\circ}\text{C}$  and stirred vigorously.  $\text{HNO}_3$  was mostly evaporated after *ca.* 20 min of stirring, and then the temperature of the oil was raised to  $200\text{ }^{\circ}\text{C}$ . The mixture was stirred with a glass rod for an additional 30 min after no smoke was observed. Cel-cat was obtained as a dark brown powder in 1.3 g (65 wt% yield).

### Mercerization of cellulose

2.0 g of Avicel was added to 40 mL of an 18 wt%  $\text{NaOH}$  aqueous solution in a centrifugation tube made of polypropylene. It was shaken initially and then aged at  $25\text{ }^{\circ}\text{C}$  for 20 min. The mixture was centrifuged, and the supernatant was removed. Using the centrifugation technique, the resulting solid was washed with 40 mL of water three times, 1% acetic acid aq. two times and again water three times. The obtained sample was dried at  $70\text{ }^{\circ}\text{C}$  in an oven. This sample was named Avicel- $\text{M}_{25}$ . The subscript number indicates the temperature of the base treatment. Mercerization was also performed in an ice bath ( $0\text{ }^{\circ}\text{C}$ ), a freezer ( $-28\text{ }^{\circ}\text{C}$ ) and a liquid nitrogen bath ( $-196\text{ }^{\circ}\text{C}$ ) for 24 h after the aging at  $25\text{ }^{\circ}\text{C}$ , and the samples produced were named Avicel- $\text{M}_0$ , Avicel- $\text{M}_{28}$  and Avicel- $\text{M}_{196}$ . Note that  $-28\text{ }^{\circ}\text{C}$  is the liquidus temperature of 18 wt%  $\text{NaOH}$  aq.<sup>11</sup> A scheme for the preparation of the most important sample (Avicel- $\text{M}_{28}$ ) is illustrated below (Fig. 2).

### Hydrolysis of cellulose

The hydrolysis of cellulose was performed in an SUS316 high pressure reactor (OM Lab-Tech, MMJ-100, 100 mL). 324 mg of a cellulose sample, 50 mg of Cel-cat and 40 mL of water were charged in the reactor. The mixture was heated from r.t. to  $230\text{ }^{\circ}\text{C}$  in 17 min, and after reaching  $230\text{ }^{\circ}\text{C}$  it was immediately cooled to r.t. by blowing air. This protocol is called the rapid heating-cooling condition.<sup>12</sup> The suspension sample was separated into solid and liquid phases by centrifugation at 5000 rpm for 10 min. The liquid part was analysed using a high-performance liquid chromatograph (HPLC; Prominence, Shimadzu) equipped with

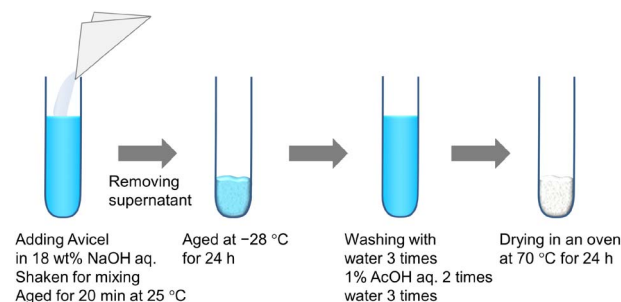


Fig. 2 Schematic for the preparation of Avicel- $\text{M}_{28}$ .



a Shodex Sugar SH-1011 column (7.8 mm × 300 mm) and a refractive index detector (RID). A typical chromatogram is shown in Fig. S1. The yield of the product was calculated with eqn (1). The solid part was dried in an oven at 70 °C and weighed to calculate the conversion value (2).

$$\text{Yield of product (\%C)} = \frac{(\text{mole of carbon atoms in the detected amount of the product})}{(\text{mole of carbon atoms in the cellulose used})} \times 100 \quad (1)$$

$$\text{Conversion (\%)} = \left[ 1 - \frac{(\text{mass of recovered cellulose})}{(\text{initial mass of cellulose})} \right] \times 100 \quad (2)$$

### Analysis of cellulose

Solid-state  $^{13}\text{C}$  cross polarization/magic angle spinning (CP/MAS) NMR spectra were measured using an AVANCE III 400 WB spectrometer ( $^{13}\text{C}$  100 MHz, Bruker). A cellulose sample was packed in a 4.0 mm zirconia rotor and rotated at 10 kHz. The spectra were calibrated using the carbonyl carbon of  $\alpha$ -glycine at 176.5 ppm as an external standard.<sup>13</sup>

Nitrogen adsorption–desorption isotherms were measured at  $-196$  °C with a BELSORP MAX X analyzer (MicrotracBEL). The samples were pre-dried overnight at 70 °C, then placed in the instrument and dried at 70 °C for 24 h prior to operation. The specific surface area was calculated by the Brunauer–Emmett–Teller (BET) method.

The morphology of cellulose particles was observed using a scanning electron microscope (SEM; JCM-7000, JEOL) at an operating voltage of 15.0 kV under the high vacuum mode. The samples were placed on the stage using carbon tape, and sputtered with gold before the measurements to reduce the charge-up effect.

Powder XRD patterns of the cellulose samples were collected on an Ultima IV X-ray diffractometer (Rigaku) attached with a D/teX Ultra2 detector using Cu K $\alpha$  radiation with a wavelength of 0.1542 nm (operation voltage 40 kV, current 40 mA) at a scan rate of 4° min $^{-1}$ .

## Results and discussion

### Effects of mercerization temperature on hydrolysis reactivity

The reactivities of Avicel and the sample mercerized at a typical temperature of 25 °C (Avicel-M<sub>25</sub>) were examined in the hydrolysis reaction (Fig. 3). The artificial catalyst named Cel-cat was used for this objective as it is one of the most active catalysts designed for crystalline cellulose hydrolysis.<sup>10,14</sup> The hydrolysis of pristine Avicel gave glucose in 22 %C yield. Other identified products were cello-oligosaccharides (1.0 %C), isomerized sugars (*i.e.* fructose and mannose; 1.8 %C), levoglucosan (1.6 %C) and 5-hydroxymethylfurfural (5-HMF; 2.9 %C). The reaction of Avicel-M<sub>25</sub> enhanced the glucose yield to 34 %C. The transformation of the crystalline structure from cellulose I to cellulose II increases the reactivity, which is discussed using the characterization data in the following section. This improvement is consistent with that observed in previous studies using enzymes and sulphuric acid.<sup>15</sup>

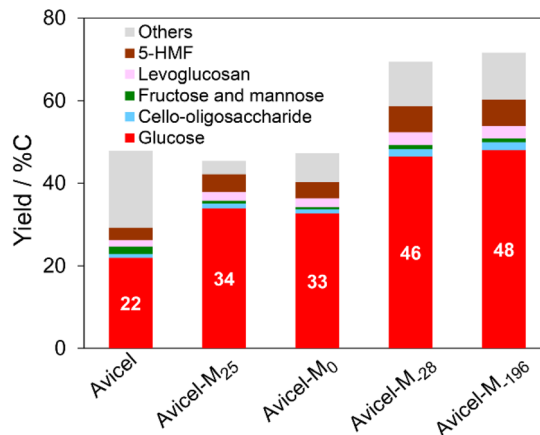


Fig. 3 Hydrolysis of pristine and mercerized cellulose samples. Cellulose 324 mg, Cel-cat 50 mg, water 40 mL, 230 °C rapid heating–cooling condition. 5-HMF: 5-hydroxymethylfurfural.

We found that the mercerization temperature affects the reactivity (Fig. 3). By decreasing the mercerization temperature from 25 °C to 0 (Avicel-M<sub>0</sub>),  $-28$  °C (Avicel-M<sub>28</sub>) and  $-196$  °C (Avicel-M<sub>196</sub>), the resulting samples gave higher yields of glucose up to 48 %C. Thus, the glucose yield was increased 2.2 times from 22 %C (pristine Avicel) by the cold base treatment. A sudden jump was observed between 0 and  $-28$  °C (33 %C and 46 %C yields, respectively). Accordingly, the reactivity of cellulose can be further improved by just decreasing the temperature of the practical pretreatment technique.

Controlled experiments were performed to clarify what conditions make cellulose reactive (Fig. S2 and Table S1). They indicated that cooling cellulose in its swollen state in the presence of NaOH is essential for improving reactivity. First, after soaking Avicel in NaOH aq. at room temperature, the swollen cellulose was separated by centrifugation and decantation and remaining NaOH solution was absorbed by pressing the sample between paper sheets. The resulting sample with no external aqueous phase was placed in a freezer at  $-28$  °C (corresponding to sample no. S3 in Fig. S2). This sample showed almost the same reactivity as Avicel-M<sub>28</sub> (glucose yield 46 %C; Table S1, entry S3). Thus, no solution phase is needed to enhance reactivity. Note that the cooling effect for completely dried samples could not be evaluated. Drying the cellulose sample swollen with NaOH aq. at room temperature caused side-reactions of cellulose, as evidenced by a colour change to yellow. In contrast to cooling in the presence of NaOH, after mercerization at room temperature, the wet sample was washed with water, acetic acid and water and then the resulting swollen material was kept at  $-28$  °C (Fig. S2, no. S2). This sample showed a similar reactivity to Avicel-M<sub>25</sub> (glucose yield 32 %C; Table S1, entry S2), *viz.* no enhancement by cooling. Likewise, Avicel treated in water at  $-28$  °C showed no improvement in reactivity (Fig. S2, Avicel<sub>28</sub>). NaOH is needed at low temperature to improve the reactivity.

### Characterization of mercerized samples

Cellulose samples were characterized to clarify the predominant factor determining their reactivity. Initially, crystalline



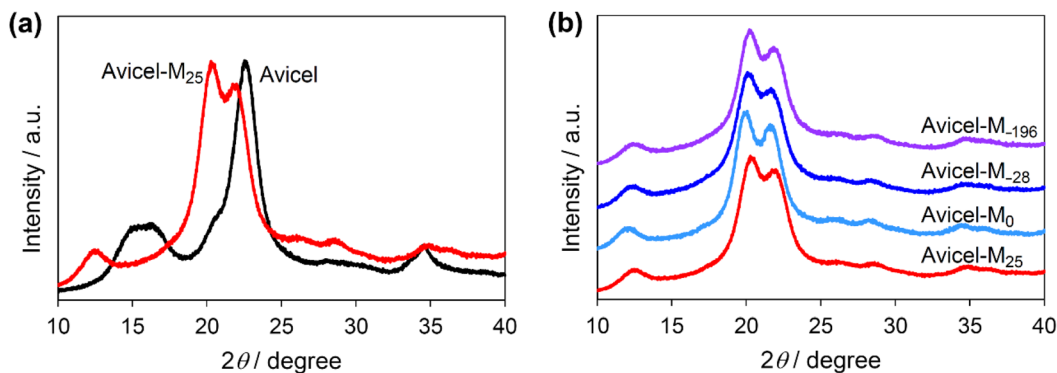


Fig. 4 XRD patterns of cellulose samples. (a) Avicel (black) and Avicel-M<sub>25</sub> (red). (b) Mercerized cellulose prepared at different temperatures.

structures of Avicel and Avicel-M<sub>25</sub> were compared using XRD (Fig. 4a). Avicel gave diffraction lines at 15° ( $1\bar{1}0$ ), 17° (110), 20.5° [(012) and (102)] and 22.5° (200), assignable to the cellulose I crystalline structure.<sup>16</sup> Cellulose I also shows a peak at 34.5°, which is often ascribed to (004), yet it is actually a mixture of several diffraction lines.<sup>16</sup> The crystallite size was 3.9 nm, determined by the Scherrer equation. On the other hand, Avicel-M<sub>25</sub> showed a diffraction pattern of cellulose II as expected: 12° ( $1\bar{1}0$ ), 20.0° (110), 22.0° (020).<sup>16</sup> The crystallite size was 5.1 nm, which was rather larger than that of Avicel. The change in crystallite size is commonly observed; cellulose molecules in multiple cellulose I crystallites likely mix to form cellulose II crystallites.<sup>17,18</sup> The ratios of crystalline and amorphous parts

were similar to each other (crystallinity index *ca.* 80%), as seen from their similar halo and diffraction line intensities.

As for the mercerized samples prepared at different temperatures, their diffraction patterns showed marginal differences (Fig. 4b). The slight shift in the diffraction angle was due to eccentric errors. The XRD analysis of cellulose mainly reflects the stacking structures of cellulose molecules, and therefore, the mercerization temperature does not affect the macroscopic molecular order significantly.

Even though the macroscopic molecular arrangement is similar, the microscopic hydrogen bonding structure could be changed at different mercerization temperatures. Therefore, we applied <sup>13</sup>C CP/MAS NMR to clarify this point (Fig. 5a), where

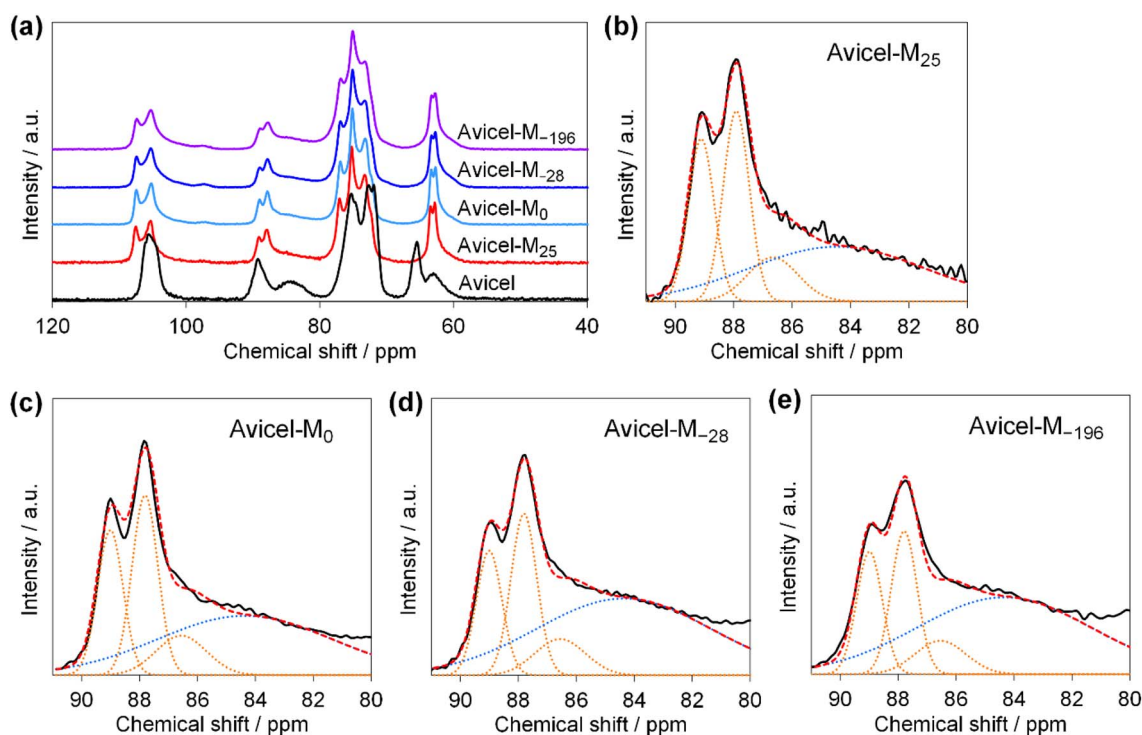


Fig. 5 (a) <sup>13</sup>C CP/MAS NMR of Avicel and mercerized samples. (b)–(e) C4 peak deconvolution for mercerized samples. Black solid line: original data; yellow dotted lines: fitting for the crystalline region; blue dotted line: fitting for the amorphous region; red dashed line: the sum of fitting curves. For the deconvolution, the same peak positions and half width were used for all data.



the C4 peak for cellulose is sensitive to the hydrogen bonding structures.<sup>19</sup> Initially, we analysed Avicel as a standard sample. It gave NMR signals for C6 at 66 ppm, C2, 3, 5 at 70–78 ppm, C4 at 89 ppm and C1 at 106 ppm, which were assigned to the cellulose I crystal. The broad peaks at 63 and 84 ppm are assignable to C6 and C4 in amorphous cellulose, respectively.<sup>20,21</sup> This result suggests a larger fraction of amorphous region (*ca.* 40%), compared to the XRD analysis. The amorphous cellulose detected in this NMR analysis reflects the cellulose molecules having a disordered hydrogen bonding structure, rather than macroscopic molecular order. Therefore, as described above, the crystallinity in <sup>13</sup>C NMR and XRD analyses is not necessarily consistent with each other.

The mercerized samples were analysed by <sup>13</sup>C NMR. They showed signals for C1 at 105–100 ppm, C4 at 80–90 ppm, C2, 3, 5 at 70–80 ppm and C6 at 60–65 ppm, which were characteristics of cellulose II (Fig. 5a). The peak splitting for each carbon is due to the presence of two topologically inequivalent glucose units in cellulose II.<sup>22</sup> For the C4 region, the two major peaks at 89.1 and 87.9 ppm are derived from the crystalline part.<sup>21,23</sup> Note that the peak positions are *ca.* 0.5 ppm higher than those in previous reports due to the revised chemical shift of the standard ( $\alpha$ -glycine carbonyl C: new 176.5 ppm, conventional 176.0 ppm).<sup>13</sup> A broad peak corresponding to the amorphous region appears at 84.5 ppm, similar to pristine Avicel. In addition, accessible surface cellulose in the crystalline region may exist at 86.7 ppm, although it is invisible.<sup>21</sup> They were overlapped, and therefore the data were deconvoluted by Gaussian functions (Fig. 5b–e). To avoid arbitrary fitting, we used the same peak positions and standard deviation values for all data. As shown in the graphs, this fitting successfully reproduced the original data. The error around 80 ppm increased as the mercerization temperature decreased, which was due to overlap with the tails of the broadened C2, 3, and 5 peaks. The peak area ratios of amorphous to crystalline cellulose ( $I_{\text{am/cry}}$ ) were 0.84, 0.99, 1.5 and 1.6 for Avicel-M<sub>25</sub>, -M<sub>0</sub>, -M<sub>28</sub> and -M<sub>196</sub>, respectively (Fig. 6a). As a side note, the fitting parameter affected the absolute values of  $I_{\text{am/cry}}$ , but the relative trend did not change. Accordingly, NaOH disarranges the hydrogen bonding structure of cellulose at  $-28$  °C or lower.

The disruption of hydrogen bonds at low temperatures could be rationalized from thermodynamics. Cellulose possesses many hydrogen bonds, and such multisite interactions stabilize the structure not only by enthalpy but also by entropy, similar to the chelate effect.<sup>14</sup> As the contribution of entropy to Gibbs energy decreases by lowering temperatures ( $\Delta_r G^\circ = \Delta_r H^\circ - T\Delta_r S^\circ$ ), a low temperature is beneficial to facilitate the penetration of hydrated Na<sup>+</sup> and OH<sup>-</sup> ions into the structure with dissociating hydrogen bonds. Analogous to this hypothesis, it is known that a concentrated HCl aqueous solution below  $-20$  °C can dissolve cellulose by dissociating the hydrogen bonding network. Furthermore,  $-28$  °C is the liquidus temperature of 18 wt% NaOH aqueous solution,<sup>11</sup> where a small fraction of liquid phase starts to freeze. Forming ice ejects solutes (namely Na<sup>+</sup> and OH<sup>-</sup>) outside with non-freezing bound water molecules on the cellulose surface, which have good mobility.<sup>24</sup> These less hydrated and mobile ions may more easily cleave the hydrogen bonds of cellulose. Accordingly, a low temperature is beneficial for cleaving the hydrogen bonds of cellulose.

We plotted the relationship between  $I_{\text{am/cry}}$  and the glucose yield in the hydrolysis reaction for the mercerized cellulose samples (Fig. 6b). This plot shows a good correlation between the two factors. It is obvious that the cold base treatment disrupts the hydrogen bonds of crystalline cellulose and improves its reactivity.

The morphology of cellulose particles was observed with an SEM (Fig. S3 and S4). Avicel had short-needle like shapes with *ca.* 100  $\mu\text{m}$  length and 20  $\mu\text{m}$  width. Mercerization at room temperature did not change the morphology significantly. Below 0 °C, cellulose particles were rather agglomerated. Accordingly, the particle shape did not show a clear relationship with reactivity.

We also measured the BET surface area of the cellulose samples by N<sub>2</sub> adsorption (Table S2 and Fig. S5). Avicel had 1.0 m<sup>2</sup> g<sup>-1</sup> of specific surface area and it increased to 1.2 m<sup>2</sup> g<sup>-1</sup> after mercerization at 25 °C. However, the cellulose samples mercerized at lower temperatures produced software errors during the measurements due to the very low adsorption volume of N<sub>2</sub> (corresponding to less than 1 m<sup>2</sup> g<sup>-1</sup> of specific surface area). A previous study suggested that a freezing

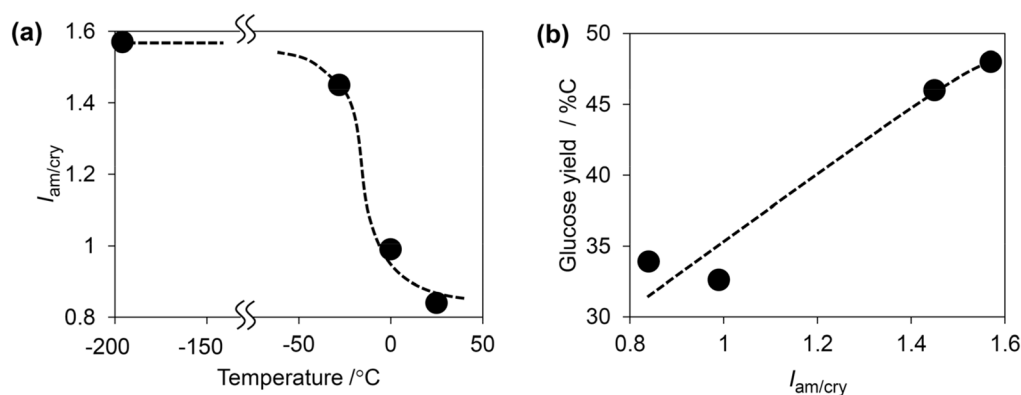


Fig. 6 (a) Effect of mercerization temperature on amorphous/crystal ratios ( $I_{\text{am/cry}}$ ). (b) The relationship between  $I_{\text{am/cry}}$  and the glucose yield during the hydrolysis reaction. The dashed lines highlight the trends.



treatment for wet agricultural waste expands its particles due to the volume change between water and ice, resulting in an increased surface area.<sup>12</sup> However, this is not the case for the cellulose samples. The improved reactivity is not attributed to the physical fracture by ice formation.

Overall, disruption of the hydrogen bonding structure is the only reasonable cause of the improved reactivity. As mentioned above, a low temperature is effective for this purpose to overcome the entropic stabilization of crystalline cellulose. Even after washing and drying, this disorder remains, resulting in enhanced cellulose reactivity.

## Conclusions

To improve the reactivity of natural crystalline cellulose, the effect of mercerization temperature was studied. This work indicates that the transformation of cellulose I to cellulose II increases its reactivity and, moreover, the gain is maximized by decreasing the treating temperature below  $-28\text{ }^{\circ}\text{C}$ . Comparing the pristine cellulose I sample and the cellulose samples after the low-temperature mercerization, glucose yield was increased by 2.2 times. Characterization of the cellulose samples showed that the low-temperature mercerization yields a structure maintaining the macro-scale molecular order of cellulose II but with a disordered hydrogen bonding network as indicated by the crystal/non-crystal ratio obtained from  $^{13}\text{C}$  NMR spectroscopy. Accordingly, just decreasing the temperature of the facile commercial method efficiently increases the reactivity of cellulose.

## Author contributions

Naomi Nishimura: methodology, investigation, visualization, writing – original draft; Yoichi Masui: investigation; Ryo Shimane: investigation, writing – review and editing; Shunsaku Yasumura: investigation; Tomohiro Iwai: methodology; Masaru Ogura: methodology, resources; Hirokazu Kobayashi: conceptualization, funding acquisition, methodology, visualization, formal analysis, supervision, writing – review and editing.

## Conflicts of interest

There are no conflicts to declare.

## Data availability

The data that support the findings of this work are available from the corresponding author upon reasonable request.

Supplementary information (SI): additional reaction data, an HPLC chart, SEM images, BET data. See DOI: <https://doi.org/10.1039/d5su00951k>.

## Acknowledgements

This work was supported by the Japan Science and Technology Agency PRESTO (Grant Number JPMJPR22N5). A part of this

work was performed in the class “Advanced Science” organized by the Komaba Institute for Science.

## Notes and references

- (a) W. Deng, Y. Feng, J. Fu, H. Guo, Y. Guo, B. Han, Z. Jiang, L. Kong, C. Li, H. Liu, P. T. T. Nguyen, P. Ren, F. Wang, S. Wang, Y. Wang, Y. Wang, S. S. Wong, K. Yan, N. Yan, X. Yang, Y. Zhang, Z. Zhang, X. Zeng and H. Zhou, *Green Energy Environ.*, 2023, **8**, 10–114; (b) S. Takkellapati, T. Li and M. A. Gonzalez, *Clean Technol. Environ. Policy*, 2018, **20**, 1615–1630; (c) H. Kobayashi and A. Fukuoka, *Green Chem.*, 2013, **15**, 1740–1763.
- R. Rinaldi and F. Schüth, *ChemSusChem*, 2009, **2**, 1096–1107.
- Y. Nishiyama, P. Langan and H. Chanzy, *J. Am. Chem. Soc.*, 2002, **124**, 9074–9082.
- A. Isogai and R. H. Atalla, *Cellulose*, 1998, **5**, 309–319.
- P. Langan, Y. Nishiyama and H. Chanzy, *J. Am. Chem. Soc.*, 1999, **121**, 9940–9946.
- C. L. Luchese, J. B. Engel and I. C. Tessaro, *Korean J. Chem. Eng.*, 2024, **41**, 571–578.
- C. Cuissinat and P. Navard, *Macromol. Symp.*, 2006, **244**, 19–30.
- T. C. Su and Z. Fang, *ACS Sustainable Chem. Eng.*, 2017, **5**, 5166–5174.
- L. Cao, J. Zhu, B. Deng, F. Zeng, S. Wang, Y. Ma, C. Qin and S. Yao, *Front. Energy Res.*, 2022, **10**, 851543.
- H. Kobayashi, R. Shimane, N. Nishimura and T. Iwai, *ACS Sustainable Resour. Manage.*, 2025, **2**, 546–553.
- M. Egal, T. Budtova and P. Navard, *Biomacromolecules*, 2007, **8**, 2282–2287.
- H. Kobayashi, T. Komanoya, K. Hara and A. Fukuoka, *ChemSusChem*, 2010, **3**, 440–443.
- M. Potrzebowski, P. Tekely, Y. Dusaosoy and F. Francé, *Solid State Nucl. Magn. Reson.*, 1998, **11**, 253–257.
- H. Kobayashi, L. Gu and N. Nishimura, *ACS Sustainable Resour. Manage.*, 2025, **2**, 1822–1824.
- D. Ciolacu, S. Gorgieva, D. Tampu and V. Kokol, *Cellulose*, 2011, **18**, 1527–1541.
- S. Nam, A. D. French, B. D. Condon and M. Concha, *Carbohydr. Polym.*, 2016, **135**, 1–9.
- H. Nishimura and A. Sarko, *J. Appl. Polym. Sci.*, 1987, **33**, 855–866.
- J. F. Revol, A. Dietrich and D. A. I. Goring, *Can. J. Chem.*, 1987, **65**, 1724–1725.
- K. Kamide, K. Okajima, K. Kowsaka and T. O. Matsui, *Polym. J.*, 1985, **17**, 701–706.
- R. H. Newman and T. C. Davidson, *Cellulose*, 2004, **11**, 23–32.
- G. Zuckerstätter, N. Terinte, H. Sixta and K. C. Schuster, *Carbohydr. Polym.*, 2013, **93**, 122–128.
- D. H. Brouwer and J. G. Mikolajewski, *Cellulose*, 2025, **32**, 4143–4160.
- S. Nomura, Y. Kugo and T. Erata, *Cellulose*, 2020, **27**, 3553–3563.
- H. O'Neill, S. V. Pingali, L. Petridis, J. He, E. Mamontov, L. Hong, V. Urban, B. Evans, P. Langan, J. C. Smith and B. H. Davison, *Sci. Rep.*, 2017, **7**, 11840.

